Ab Initio Study of Acrylate Polymerization Reactions: Methyl Methacrylate and Methyl Acrylate Propagation

Xinrui Yu, Jim Pfaendtner, and Linda J. Broadbelt*

Department of Chemical and Biological Engineering, Northwestern University, Evanston Illinois 60208-3120

Received: January 22, 2008; Revised Manuscript Received: May 8, 2008

The kinetic parameters of the free radical propagation of methyl methacrylate and methyl acrylate have been calculated using quantum chemistry and transition state theory. Multiple density functional theory (DFT) methods were used to calculate the activation energy, and it was found that MPWB1K/6-31G(d,p) yields results that are in very good agreement with experimental data. To obtain values of the kinetic parameters that were in the best agreement with experimental data, low frequencies were treated using a one-dimensional internal rotor model. Chain length effects were also explored by examining addition reactions of monomeric, dimeric, and trimeric radicals to monomer for both methyl methacrylate and methyl acrylate. The results show that the values for the addition of the trimeric radical to monomer are closest to experimental data. The kinetic parameters that were calculated using a continuum description of the monomer as a solvent were not significantly different from the vacuum results.

1. Introduction

Free radical polymerization is the main approach to produce acrylate polymers for automobile coating resins. Traditional solvent-borne acrylic resins consist of high molecular weight polymers, which need a high content of volatile organic solvent (70%) to be processed as coatings.[1,2] Driven by environmental considerations, novel resins consisting of low molecular weight oligomers with cross-linkable functional groups have been unfurled as the new generation of resin coatings.[1,3] These prepolymers can undergo cross-linking reactions on metal surfaces with an added curing agent to form a robust firm coating layer. Polymerization at high temperature (>120 °C) is an economical way to produce such prepolymers, which essentially prompts some secondary reactions such as transfer and scission reactions to produce low molecular weight resins.[4]

Free radical polymerization is a complex process. Propagation is the main reaction to increase chain length, in which long chain radicals add to unsaturated bonds of the monomer, as illustrated in Figure 1 for methyl methacrylate and methyl acrylate. At high temperatures, secondary reactions such as transfer and scission can be significant.[5–7] A quantitative description of acrylate polymerization would require that rate parameters be known for all of the different reactions comprising the reaction mechanism. However, it is very difficult to measure kinetic parameters for individual reactions experimentally because these reactions are coupled. With the advent of pulsed laser polymerization in combination with size exclusion chromatography (PLP-SEC), direct measurement of propagation rate constants (k_p) is feasible.[8–11] PLP-SEC controls radical generation and termination by successive irradiation of photoinitiators using a laser, and rate coefficients can be determined on the basis of measuring the chain length and time interval between pulses. However, measurement of k_p for polymerization reactions is confounded when transfer or other reactions are significant between laser pulses.[9,10] In addition, PLP-SEC can be used to measure k_p and termination rate coefficients (k_t) of homopolymerization without having to assume any model.[12–14] However, PLP-SEC needs to be used in combination with polymerization models if rate coefficients relevant to copolymerization and some secondary reactions such as depropagation are desired.[15,16] Although electron spin resonance (ESR) and nuclear magnetic resonance (NMR) can corroborate the presence of secondary reactions such as transfer and scission,[17,18] their rate constants can only be estimated in the context of a model.

It is thus valuable to have alternative methods for specifying rate coefficients of the elementary steps composing polymerization. In particular, the use of quantum chemistry to calculate rate coefficients in free radical polymerization systems is particularly attractive.[19] Computational chemistry can be applied to any reaction type, and extracting quantitative values of rate coefficients does not rely on assuming a polymerization model such as the terminal or penultimate models commonly used in copolymerization. With the development of computational quantum chemistry, obtaining accurate kinetic parameters via a computational approach is feasible, especially for reactions of small molecules.[20–22] Recently, this approach has been extended to the determination of polymerization reactions. However, these studies have focused on small monomers such as ethylene, vinyl chloride, acrylonitrile, and methacrylonitrile.[23–26] Nevertheless, this body of work provides guidance about the different choices that must be made and which assumptions are reasonable when quantitatively accurate values of rate coefficients in polymerization are sought. Heuts and Gilbert and Van Cauter et al. studied radical addition reactions of ethlyene using quantum chemical calculations.[23,24] Heuts and Gilbert used a relatively low level method, HF/3-21G, to optimize geometries on the basis of the conclusion that geometry is not sensitive to the method and basis set. A high level method, QCISD(T)/6-311G(d,p), was used to calculate the activation energy,[23] and an artificial heavy atom was used on the chain end to simulate the presence of a long chain. Van Cauter et al. used B3LYP/6-31G(d) for both geometry optimization and calculation of the energies. The influence of chain length was studied by increasing the radical chain length to 15. Both sets of researchers went beyond the rigid-rotor, harmonic oscillator (HO) approximation

* Corresponding author. Phone: (847) 491-5351; e-mail: broadbelt@northwestern.edu.

10.1021/jp800643a CCC: $40.75
Published on Web 06/28/2008

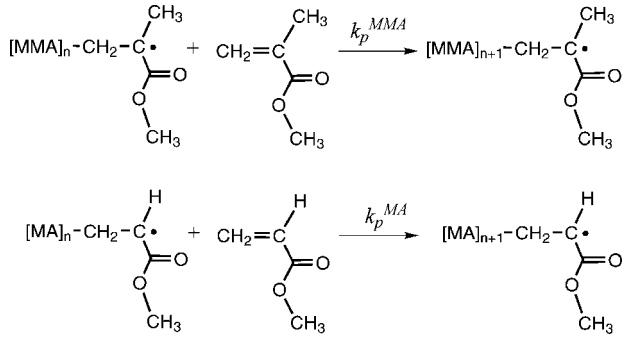

Figure 1. Methyl methacrylate and methyl acrylate propagation reactions.

and treated low frequency modes as internal rotations. Van Cauter and co-workers analyzed the difference between the results obtained when one-dimensional and two-dimensional hindered rotor (HR) models were used and found that these two treatments only differed slightly due to fortuitous cancelation of errors in the one-dimensional approach. Izgorodina and Coote studied the homopolymerization of acrylonitrile and vinyl chloride.[25] Geometry optimization was performed using B3LYP/6−31G(d), and the influence of the calculation method on the activation energy for k_p was probed for various methods, including density functional theory (DFT) (B-LYP, B3LYP, MPWB1B95, BB1K, MPWB1K), ROMP2 with a basis set of 6-311+G(3df,3p), and the hybrid ONIOM method. Polymeric radicals only as large as three units long were studied, and low frequencies were treated using a one-dimensional internal rotor model.

In the present work, we extended this general approach to calculate k_p for larger monomers, methyl methacrylate and methyl acrylate. Because of the size of the reaction systems, DFT was used for all calculations, which has been shown to provide a compromise between computational time and accuracy in previous research.[19,24,25,27,28] Geometry optimization, location of transition states, and potential energy scans for treatment of internal rotations were all based on unrestricted B3LYP/6-31G(d). B3LYP with five different basis sets (6-31G(d), 6-31G(d,p), 6-311G(d,p), 6-311+G(d,p), and 6-311G(3df,2p)), and MPWB1K/6-31G(d,p) and B1B95/6-31G(d,p) were used in order to investigate the influence of DFT method and basis set on the electronic energy. The results from the HO model and internal rotation treatment were contrasted. Activation energies and frequency factors were regressed from ln k versus $1/T$ over a temperature range of 298.15 to 800 K, and the calculated data were benchmarked against the experimental data of Buback et al., who measured k_p for methyl methacrylate between −1 °C and 90 °C using PLP-SEC as reported in eq 1,[8]

$$k_p^{MMA}(\mathrm{L \cdot mol^{-1} \cdot s^{-1}}) = 2.67 \times 10^6 \exp\left(\frac{-22.4(\mathrm{kJ \cdot mol^{-1}})}{RT}\right) \quad (1)$$

and k_p for methyl acrylate between −19 °C and 32 °C as reported in eq 2,[9]

$$k_p^{MA}(\mathrm{L \cdot mol^{-1} \cdot s^{-1}}) = 1.66 \times 10^7 \exp\left(\frac{-17.7(\mathrm{kJ \cdot mol^{-1}})}{RT}\right) \quad (2)$$

The goal of this work was to develop a computational methodology to study acrylate polymerization reactions that is quantitatively accurate yet computationally affordable. Given the validation of the present results against experimental data, the methodology can then be extended with confidence to other reactions in acrylate systems, including copolymerization and side reactions such as transfer and scission.

2. Method and Computational Details

Propagation of methyl methacrylate and methyl acrylate was studied using the addition of monomeric, dimeric, and trimeric radicals to monomer, as shown in Figure 2. Gaussian 03 was used for all of the calculations.[29] All the reactants and products were first optimized with unrestricted B3LYP/6-31G(d) using the keyword *"opt"* via conventional gradient-based optimization.[30,31] However, the optimized geometry is dependent on the initial structure provided as input, particularly for large species with many degrees of freedom. Although a Boltzmann distribution of low energy conformers will exist during reaction, we sought to find the lowest energy conformations for the reactants and the products. In order to overcome the barriers between "local" minimum conformations and locate "global" minimum conformations, potential energy scans were performed for each single bond in the optimal structure identified by conventional optimization. Unrestricted B3LYP/6-31G(d) was also used for all potential scans. If lower energy conformers were identified, a new set of potential energy scans was carried out until no conformations of lower energy were obtained. Although one-dimensional torsional scans do not guarantee that the global minimum will be located, much of the variation in conformations is derived from torsional motions around single bonds, and our approach did indeed often identify conformations that were lower in energy than the one obtained by conventional optimization. While the use of coupled scans in two dimensions or higher may have identified conformations of even lower energy, the computational cost was prohibitive for the size of species investigated here.

To locate transition state structures, the QST3 method was used, which requires the optimized reactants, product, and an estimate of the transition state.[32] Because all the addition reactions follow the same basic reaction path, i.e., addition of the radical center to the unsaturated C═C bond of the monomer, the estimated transition state was constructed by elongating the carbon−carbon single bond in the β-position to the radical center of the addition product to a bond length of 2.3 Å. Transition states were identified as saddle points on the potential energy surface, possessing one imaginary frequency. Once possible transition state structures were identified, they were verified using intrinsic reaction coordinate (IRC) following with a step size of 0.1 amu$^{0.5}$-Bohr. Unrestricted B3LYP/6-31G(d) was used for both the QST3 and the IRC calculations. Frequencies were also calculated using unrestricted B3LYP/6-31G(d), and the zero-point vibrational energy (ZPVE) was calculated using a scale factor of 0.9806.[33] A scale factor of 1.0002 was used in the calculation of partition functions based on the recommended scale factors for ΔH_{vib} and ΔS_{vib} reported by Scott and Radom.[33]

With the optimized structures in hand, the electronic energy, E_e, was obtained from single point calculations using unrestricted B3LYP with five different basis sets (6-31G(d), 6-31G(d,p), 6-311G(d,p), 6-311+G(d,p), and 6-311G(3df,2p)), MPWB1K/6-31G(d,p), which was optimized against barrier heights based on nine elementary reactions by Truhlar et al.,[34] and B1B95/6−31G(d,p)[35] for both methyl methacrylate and methyl acrylate. In addition to the gas phase values calculated, their application to condensed phase chemistry was evaluated using a polarizable continuum model (PCM), in which the solvent was treated as a polarizable continuum, and the solute was placed in a cavity

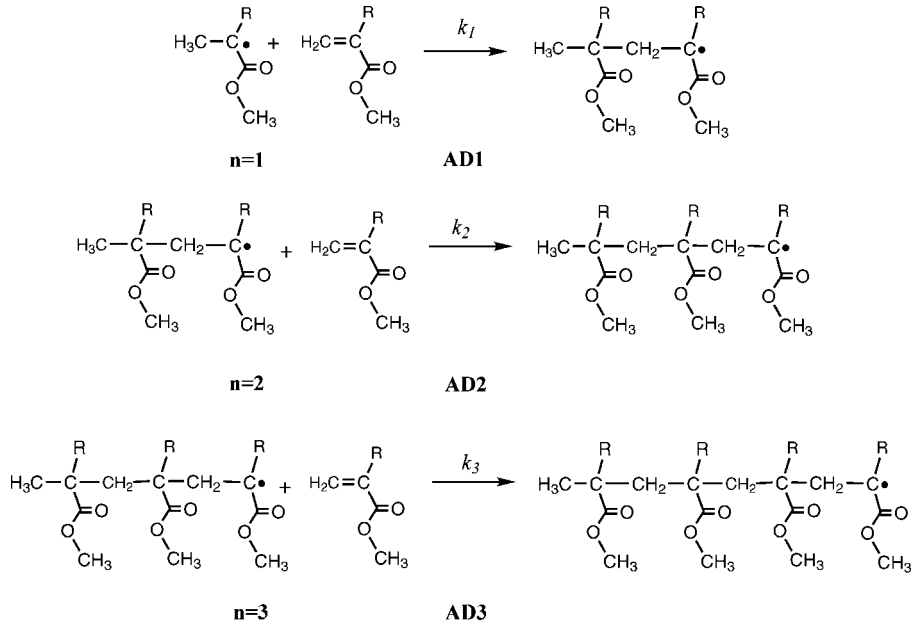

Figure 2. Methyl methacrylate and methyl acrylate addition reactions were studied as a function of chain length, AD*n* is used to denote the different calculations performed, where *n* is the number of monomeric units in the radical reactant. For methyl methacrylate, R is a CH_3 group, and for methyl acrylate, R is a hydrogen atom.

within the solvent.[36] Dielectric constants of methyl methacrylate (ε) equal to 6.32 and methyl acrylate (ε) equal to 7.03 were used to simulate the bulk reaction environment.[37] Reaction rate constants for propagation were then calculated using eq 3 at a series of temperatures from 298.15 to 800 K based on transition state theory:[38]

$$k(T) = \kappa(T)\frac{k_B T}{h}(c^0)^{1-m}\frac{Q^{\ddagger}}{Q_{mon}Q_{rad}}e^{-\Delta E_0/RT} \quad (3)$$

where $\kappa(T)$ is the tunneling factor, k_B is Boltzmann's constant (1.3806×10^{-23} J·mol^{-1}·K^{-1}), h is Planck's constant (6.6261×10^{-34} J·s), m is the number of reactants, which is 2 for propagation, c^0 is the standard state concentration (mol·L^{-1}) to which the quantum chemical calculations are referenced, P/RT, where P is 1 atm, and ΔE_0 is the difference between the E_0 of the transition state and the reactants, which is defined as the summation of the electronic energy (E_e) and the ZPVE:

$$E_0 = E_e + \mathrm{ZPVE} \quad (4)$$

ZPVE is the contribution to the energy from vibration at 0 K as defined in eq 5:[39]

$$\mathrm{ZPVE} = \frac{1}{2}\sum_{i}^{3N-6} h\nu_i \quad (5)$$

in which N is the number of atoms, and ν_i represents the frequencies. For transition states, $3N - 7$ frequencies are included in the ZPVE. The tunneling factor ($\kappa(T)$) was assumed to be one for the radical addition reactions studied here. Tunneling effects would be important in related radical reactions, such as atom transfer reactions,[28,40] and would need to be calculated explicitly such as we have done in other work studying intramolecular and intermolecular hydrogen transfer of peroxy radicals.[40,41] Arrhenius behavior was obeyed over the temperature range used to determine the kinetic parameters; R^2 was greater than 0.99 for all cases studied. Thus, k_p values at temperatures even higher than those typically practiced (<200 °C for batch polymerization; <90 °C (methyl methacrylate) and <32 °C (methyl acrylate) for PLP-SEC such that side reactions are suppressed) can be predicted.

A critical part of obtaining accurate values of $k(T)$ is specifying the values of $Q^{\ddagger}$, Q_{mon}, and Q_{rad} in eq 3, which are the partition functions for the transition state, the monomer, and the radical, respectively. The partition function is conventionally considered to include contributions from four different modes: electronic (Q_e), translation (Q_{tr}), rotation (Q_r), and vibration (Q_v), as shown in eq 6:

$$Q = Q_e Q_{tr} Q_r Q_v \quad (6)$$

For species in their ground state, $Q_e = 1$, and Q_{tr} and Q_r are defined in standard textbooks.[39] Q_v is the vibrational partition function based on the contributions from the individual frequencies, which are often calculated using the HO approximation. However, this is known to be inaccurate for some motions characterized by low frequencies, which are often better treated as hindered rotations. If there are many torsional motions with low frequencies, their contributions can be quite large, and the difference between the partition function values can be significant. To account for these hindered rotations, Q_v is expressed in eq 7 as two parts, Q_{vib} and $Q_{int,rot}$:

$$Q = Q_e Q_{tr} Q_r Q_{vib} Q_{int,rot} \quad (7)$$

where $Q_{int,rot}$ is the contribution to the partition function of the low vibrational modes that are better treated as internal rotations, and Q_{vib} is the vibrational contribution from those modes that are treated as HOs. There is no well accepted cutoff value to define "low" frequencies that should be treated as $Q_{int,rot}$. In the literature, 200 cm^{-1} was used as the upper limit to define low frequencies by some researchers,[23] while 300 cm^{-1} was used in other examples.[25] In these studies, the frequencies lower than the cutoff value were taken out of Q_v and replaced by $Q_{int,rot}$, which was calculated as the product of the partition functions of each rotor. For simple rotors whose potential can be expressed in the form of eq 8 (where W is the rotation barrier height, n is the symmetry number of rotation, and θ is the torsional angle), McClurg et al. provided an asymptotic factor

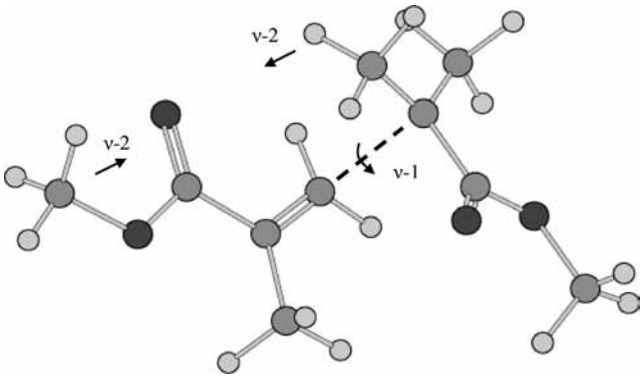

Figure 3. The transition state for the AD1 reaction of methyl methacrylate shown in Figure 2 and characteristic motions of two of its frequencies. ν-1 (20.3 cm^{-1}) is the lowest positive frequency, and it corresponds to the torsional motion about the bond defining the transition state. ν-2 (45.3 cm^{-1}) is the second lowest frequency, and it has no torsional component.

for specifying the partition function value $Q_{int,rot}$, which converges to that for a free rotor at high temperature and to an HO at low temperature.[42]

$$V(\theta) = \frac{W}{2}(1 - \cos n\theta) \tag{8}$$

However, this method is restricted to symmetric rotors and could not be used in methyl methacrylate or methyl acrylate propagation reactions.

In the present approach, we did not apply an arbitrary upper bound to define what was classified as a low frequency, and we used a method for calculating $Q_{int,rot}$ that was general for rotations of any symmetry. The number of low frequencies that were removed was set as the number of rotors, which included rotations about σ bonds and the bond defining the transition state. Although the bond defining the transition state is not a real bond, it is treated as an HR since the lowest positive frequency in the transition state mainly consists of torsional motion about this forming bond. Rather than simply removing the contribution of the N lowest frequencies from Q_{vib}, where N is the number of rotors, the low frequencies were examined to make sure they consisted of rotational components. Interestingly, all vibrational motions that were removed for all species had frequencies less than 200 cm^{-1}. For the reactants (monomer and radical) and the radical product, the lowest N frequencies all had rotational components. However, the transition states were different since some low frequencies are essentially a bending motion involving the monomer and radical. For example, as shown in Figure 3, frequency ν-2 (45.3 cm^{-1}) in the methyl methacrylate AD1 transition state involves the bending motion of the monomer and the radical. Frequencies that did not consist of torsional motions were not treated as hindered rotations and thus remained as part of the HO portion of Q_v. For those frequencies removed from Q_v, their contributions to ZPVE were also removed. The values of the frequencies of the modes that were removed were simply calculated from the original HO analysis. While approaches for calculating the "pure" frequency to which a given internal rotation corresponds have been used by McClurg and co-workers[42] and Truhlar,[43] the more straightforward approach practiced in other work was also used here.[23–26] The partition function of the mth internal rotor was calculated using eq 9:

$$Q_{int,rot,m} = \frac{1}{\sigma_m}\sum_i \exp\left(-\frac{\varepsilon_i}{k_B T}\right) \tag{9}$$

where σ_m is the symmetry number of the internal rotation, and ε_i are the energy levels of the internal rotation, which were calculated by solving a one-dimensional Schrödinger equation:

$$-\frac{\hbar^2}{2I_{red}}\frac{d^2}{d\theta^2}\Psi + V(\theta)\Psi = \varepsilon\Psi \tag{10}$$

where $\hbar$ is Planck's constant divided by 2π, Ψ is the wave function, θ is the torsional angle, and I_{red} is the reduced moment of inertia, which was defined as I,[2,3] in accord with the systematic classification of moments of inertia by East et al.[44] $V(\theta)$ was determined from relaxed potential energy scans calculated using unrestricted B3LYP/6-31G(d) using the keyword *"modredundant"* and intervals of 30°; thus, a total of 12 optimized conformations from 0° to 360° were obtained for each rotor. $V(\theta)$ was expanded using a full Fourier series as in eq 11:

$$V(\theta) = \sum_{i=1}^{n}[a_i(1 - \cos i\theta) + b_i \sin i\theta] \tag{11}$$

where a_i and b_i are the coefficients of the expansion. Equation 11 can be written in its matrix product form, and the coefficients a_i and b_i were determined by solving an overdetermined matrix. In order to ensure this matrix was overdetermined, the number of coefficients was less than the number of energy points during the rotation. For a scan interval of 30°, n was set equal to 3. This was demonstrated to be a sufficient number of coefficients to ensure acceptable fits for all potential energy scans. For example, potential energy scans for the four rotors in methyl methacrylate monomer outlined in Figure 4 are shown in Figure 5. The potential energy scans are shown as points, and the fitted curves using eq 11 are shown as the lines. The four rotors shown in Figure 4 include both symmetric rotors (e.g., methyl group) and asymmetric rotors (e.g., methoxyl group).

The one-dimensional Schrödinger equation (eq 10) was solved using the Fourier grid Hamiltonian (FGH) method, in which the Hamiltonian operator was discretized over the torsional angle range, and the energy levels, ε_i (eigenvalues), were calculated by diagonalizing the Hamiltonian matrix.[45] In this research, the Hamiltonian operator was discretized using 1000 points. Comparison of partition functions calculated for methyl methacrylate monomer showed that 1000 points gave results that were consistent with finer grids containing 5000 points; the maximum deviation was less than 1.2%, and the deviation decreased with increasing temperature, as shown in Table 1. The calculation of the reduced moment of inertia, solutions of the Fourier coefficients and the Schrödinger equation, and calculation of

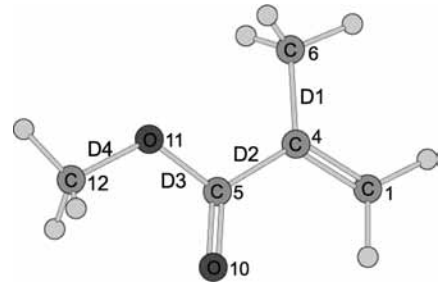

Figure 4. Potential energy scans were carried out for the four dihedral axes of methyl methacrylate monomer: D1 (C4,C6), D2 (C4,C5), D3 (C5,O11), and D4 (O11,C12).

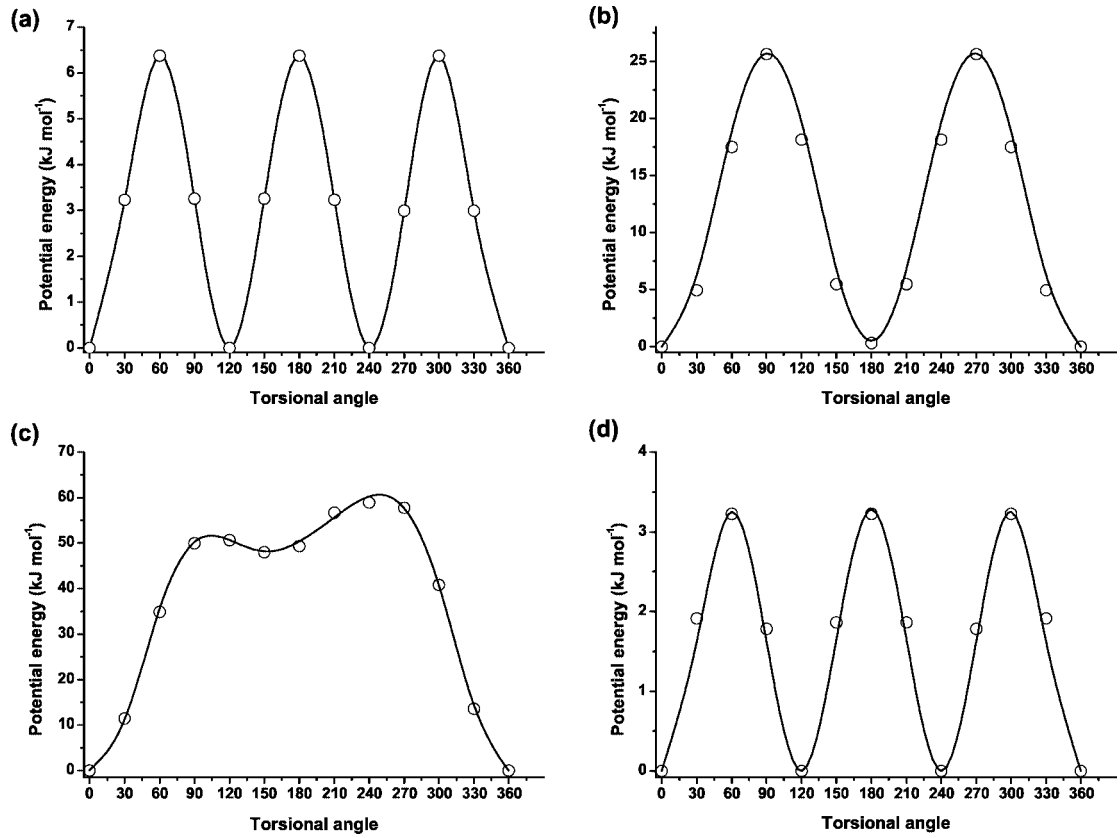

Figure 5. Potential energy scans for all the dihedrals defined for methyl methacrylate monomer in Figure 4: (a) D1, (b) D2, (c) D3, and (d) D4. The potential energy scans carried out in 30° increments using unrestricted B3LYP/6-31G(d) are shown as points, and the Fourier fits are shown as lines.

TABLE 1: $Q_{int,rot}$ of the Four Rotors of Methyl Methacrylate Monomer Defined in Figure 4 Based on a One-Dimensional Internal Rotor Model As a Function of the Number of Grid Points Used to Solve the One-Dimensional Schrödinger Equation and Temperature

	$Q_{int,rot,D1}$			$Q_{int,rot,D2}$			$Q_{int,rot,D3}$			$Q_{int,rot,D4}$		
T (K)	1000	5000	% dev.	1000	5000	% dev.	1000	5000	% dev.	1000	5000	% dev.
298.15	1.402	1.400	0.12	3.116	3.105	0.33	1.084	1.071	1.16	1.980	1.979	0.06
300	1.412	1.410	0.12	3.136	3.126	0.33	1.091	1.078	1.16	1.993	1.991	0.06
350	1.676	1.674	0.10	3.701	3.690	0.29	1.284	1.270	1.06	2.314	2.313	0.05
400	1.936	1.934	0.09	4.269	4.258	0.27	1.476	1.462	0.98	2.619	2.618	0.05
450	2.190	2.188	0.08	4.841	4.829	0.24	1.669	1.653	0.92	2.907	2.906	0.04
500	2.437	2.435	0.07	5.418	5.406	0.23	1.861	1.845	0.86	3.182	3.180	0.04
550	2.678	2.676	0.06	5.999	5.987	0.21	2.054	2.037	0.82	3.443	3.442	0.03
600	2.912	2.910	0.06	6.586	6.573	0.20	2.248	2.230	0.77	3.692	3.691	0.03
700	3.360	3.358	0.05	7.772	7.759	0.17	2.638	2.619	0.71	4.161	4.160	0.03
800	3.783	3.781	0.04	8.974	8.960	0.15	3.035	3.015	0.65	4.595	4.594	0.02

the partition functions was carried out with "*calck*" program developed in our group.[46,47]

3. Results and Discussion

3.1. Geometry Optimization. The bond length of the bond defining the transition state indicates the relative progress along the reaction coordinate. The transition states of the AD1 to AD3 reactions for methyl methacrylate obtained from unrestricted B3LYP/6−31G(d) are shown in Figure 6. Note that only syndiotactic attack was considered in this work. While isotactic addition is also possible, it is less favorable sterically, so only the preferred syndiotactic route was explored. The bond lengths of the bond defining the methyl methacrylate transition states of AD1, AD2, and AD3 are 2.268 Å, 2.242 Å, and 2.235 Å, respectively, which are different by less than 0.04 Å. The bond lengths of the bond defining the methyl acrylate transition states of AD1, AD2, and AD3 are 2.302 Å, 2.299 Å, and 2.296 Å, respectively, which are different by less than 0.01 Å. The dihedral angles formed by the methyl methacrylate transition state bond $C_1{=}C_2{\cdots}C_3{-}C_4$ as shown in Figure 6 are 168.5°, 174.9°, and 177.0° for AD1, AD2, and AD3, respectively, and the corresponding dihedral angles for methyl acrylate are 172.3°, 179.3°, and 174.0° for AD1, AD2, and AD3, respectively. These four carbon atoms are nearly in the same plane, which corresponds to the stable conformation of the product.

3.2. Calculation Method and Basis Set Comparison. One of the most challenging aspects of using quantum chemistry to study large molecules is to find a suitable method and basis set. This is especially important when activation energies are of interest since the reaction energy barrier is sensitive to the calculation method. Although high-level methods such as QCISD(T)/6-311G(d,p) and CBS-RAD have been used in

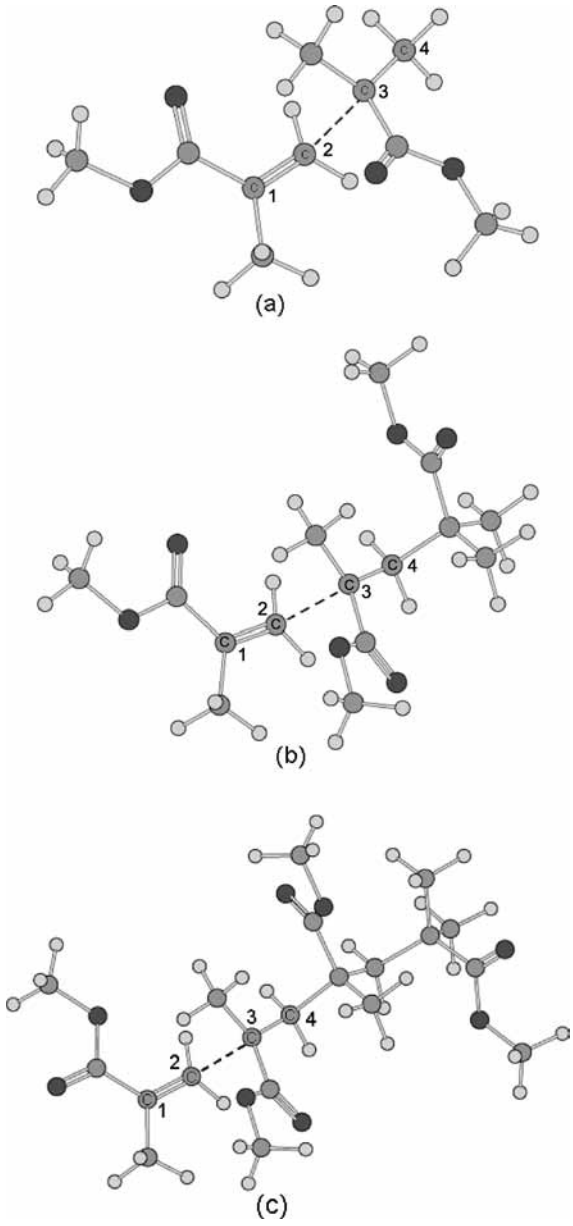

Figure 6. Transition state structures for the (a) AD1, (b) AD2, and (c) AD3 reactions of methyl methacrylate located using unrestricted B3LYP/6-31G(d).

previous research related to radical addition reactions,[19] they have been applied to relatively small reactions and are too expensive for reaction systems that involve a large number of atoms such as methyl methacrylate and methyl acrylate propagation. Since the geometry is not highly sensitive to the method/basis set, unrestricted B3LYP/6-31G(d) was used for geometry optimization, location of transition states and potential energy scans. However, the activation energy based on E_e calculated with unrestricted B3LYP/6-31G(d) was too high compared to experimental results as summarized in Table 2 and Table 3. For AD3 of methyl methacrylate, the unrestricted B3LYP/6-31G(d) activation energy is about 17 kJ·mol^{-1} higher than that from PLP-SEC. For AD3 of methyl acrylate, the unrestricted B3LYP/6-31G(d) activation energy is about 10 kJ·mol^{-1} higher than the experimental value. The use of a larger basis set does not change the results appreciably; the activation energies calculated using 6-31G(d) and 6-31G(d,p) are within 0.4 kJ·mol^{-1} for all six addition reactions of methyl methacrylate and methyl acrylate. Even larger basis sets (6-311G(d,p) and 6-311G(3df,2p)) resulted in activation energies that were in even worse agreement with the experimental values. For AD3 reactions, the activation energies calculated using B3LYP/6-311G(d,p) were 22.9 kJ·mol^{-1} and 13.9 kJ·mol^{-1} higher than the experimental values for methyl methacrylate and methyl acrylate, respectively; the calculated activation energies for methyl methacrylate AD3 with UB3LYP/6-311G(3df,2p) were 25.1 kJ·mol^{-1} and 12.2 kJ·mol^{-1} higher than the experimental data for methyl methacrylate and methyl acrylate, respectively. The addition of diffuse functions using the 6−311+G(d,p) basis set did not improve the agreement between the calculated activation energies and the experimental values.

The use of two other DFT methods, MPWB1K/6-31G(d,p) and B1B95/6-31G(d,p), to perform single-point E_e calculations for methyl methacrylate was also explored as shown in Table 2. MPWB1K was specified by using "MPWB95" with the user-defined statement "*Iop*(3/76=0560004400)" in the keyword line in Gaussian 03. As shown in Table 2, the change in the electronic energy of reaction with level of theory is very striking, which in turn translates into dramatic differences in the activation energies. The ΔE_0 values calculated using MPWB1K/6-31G(d,p) were the lowest, which were on average 15 kJ·mol^{-1} lower than those calculated using B3LYP/6-31G(d) for methyl methacrylate. The activation energy obtained using MPWB1K/6-31G(d,p) of 22.7 kJ·mol^{-1} for methyl methacrylate AD3 is the closest to the experimental E_a for methyl methacrylate propagation, which is 22.4 kJ·mol^{-1}.

MPWB1K/6-31G(d,p) and B1B95/6-31G(d,p) were also used to calculate kinetic parameters for methyl acrylate addition reactions. The results are shown in Table 3. The results in Table 3 have very similar tendencies as those reported for methyl methacrylate in Table 2. For a given AD*n* reaction, the activation energies based on E_e calculated with unrestricted B3LYP/6-31G(d) are higher than those based on MPWB1K/6-31G(d,p) and B1B95/6-31G(d,p). However, the differences are smaller compared with the corresponding reactions for methyl methacrylate. For example, for the methyl acrylate AD3 reaction, the difference between unrestricted B3LYP/6-31G(d) and MPWB1K/6-31G(d,p) is about 6 kJ·mol^{-1}, while, for the methyl methacrylate AD3 reaction, the difference is about 17 kJ·mol^{-1}. The activation energy based on MPWB1K/6-31G(d,p) for the methyl acrylate AD3 reaction with low frequencies treated using the internal rotation model (21.5 kJ·mol^{-1}) is the closest to the E_a value measured using PLP-SEC, which is 17.7 kJ·mol^{-1}, as was the case for methyl methacrylate.

It is interesting to compare the results obtained here with values reported for similar systems in the literature. Fischer and Radom measured rate coefficients for the addition of a series of radicals to vinyl monomers including methyl methacrylate and methyl acrylate.[19] None of these radicals has the same structure as either the methyl methacrylate or methyl acrylate AD1 radicals, but there are some analogous radicals. The PEst radical [$(CH_3)_3COC(O)\dot{C}(CH_3)_2$] is similar to the methyl methacrylate AD1 radical in that the radical center is tertiary. The activation energy of PEst radical addition to methyl methacrylate monomer reported was 22.4 kJ·mol^{-1}, which was calculated from the measured rate coefficient by assuming a representative frequency factor. This is close to the calculated activation energy predicted for methyl methacrylate AD1 with MPWB1K/6-31G(d,p) (27.7 kJ·mol^{-1}). They also reported the reaction of a primary ester radical, $(CH_3)_3COC(O)\dot{C}H_2$, with both methyl acrylate and methyl methacrylate and obtained values of 1.3 ± 0.3 × 10^4 mol·L^{-1}·s^{-1} and 3.5 ± 0.2 × 10^4 mol·L^{-1}·s^{-1}, respectively, at 278 K. These values are even higher than our

TABLE 2: Electronic Energy (E_e), Zero Point-Corrected Energy (E_0) of Reaction, and Activation Energy (E_a) for Both the HO and HR Models As a Function of Chain Length (AD1, AD2, and AD3 in Figure 2) for Methyl Methacrylate Propagation[a]

	UB3LYP/ 6-31G(d)	UB3LYP/ 6-31G(d,p)	UB3LYP/ 6-311G(d,p)	UB3LYP/ 6-311+G(d,p)	UB3LYP/ 6-311G(3df,2p)	MPWB1K/ 6-31G(d,p)	B1B95/ 6-31G(d,p)
AD1							
ΔE_e	23.5	23.4	27.7	32.9	30.5	12.2	23.4
ΔE_0	28.4	28.3	32.6	37.8	35.4	17.1	28.3
E_a^{HR}	38.9	38.8	43.1	48.1	46.0	27.7	38.8
E_a^{HO}	35.2	35.1	39.4	44.3	42.3	24.0	35.1
AD2							
ΔE_e	28.5	28.6	34.0	38.1	36.2	12.2	26.4
ΔE_0	33.0	33.1	38.5	42.6	40.7	16.7	30.9
E_a^{HR}	44.3	44.5	49.9	54.0	52.1	28.0	42.3
E_a^{HO}	40.3	40.4	45.8	50.0	48.2	23.9	38.2
AD3							
ΔE_e	32.1	32.1	37.8	43.0	39.9	15.2	28.4
ΔE_0	36.2	36.2	41.9	47.1	44.0	19.3	32.5
E_a^{HR}	39.6	39.6	45.3	50.5	47.5	22.7	35.9
E_a^{HO}	43.6	43.6	49.3	54.6	51.6	26.8	40.0

[a] Units: kJ·mol^{-1}. Methyl methacrylate propagation E_a obtained from PLP-SEC: 22.4 kJ·mol^{-1}. ZPVE values were calculated using UB3LYP/6-31G(d) with a scale factor of 0.9806. ZPVE(AD1) = 4.9 kJ·mol^{-1}; ZPVE(AD2) = 4.5 kJ·mol^{-1}; ZPVE(AD3) = 4.1 kJ·mol^{-1}.

TABLE 3: Electronic Energy (E_e), Zero Point-Corrected Energy (E_0) of Reaction and Activation Energy (E_a) for Both the HO and HR Models As a Function of Chain Length (AD1, AD2, and AD3 in Figure 2) for Methyl Acrylate Propagation[a]

	UB3LYP/ 6-31G(d)	UB3LYP/ 6-31G(d,p)	UB3LYP/ 6-311G(d,p)	UB3LYP/ 6-311+G(d,p)	UB3LYP/ 6-311G(3df,2p)	MPWB1K/ 6-31G(d,p)	B1B95/ 6-31G(d,p)
AD1							
ΔE_e	18.3	18.6	22.3	23.0	23.6	13.9	16.0
ΔE_0	22.7	23.0	26.7	27.4	28.0	18.3	20.4
E_a^{HR}	31.1	31.4	35.1	35.4	36.3	26.4	28.8
E_a^{HO}	30.2	30.5	34.2	34.5	35.4	25.5	27.9
AD2							
ΔE_e	16.8	17.1	21.2	21.9	21.8	10.9	14.6
ΔE_0	20.3	20.6	24.7	25.4	25.3	14.4	18.1
E_a^{HR}	28.9	29.2	33.3	34.1	33.9	22.8	26.7
E_a^{HO}	28.5	28.8	32.9	33.6	33.4	22.4	26.3
AD3							
ΔE_e	21.2	21.6	25.3	25.9	23.6	15.3	19.2
ΔE_0	24.4	24.8	28.5	29.1	26.8	18.5	22.4
E_a^{HR}	27.5	27.9	31.6	32.2	29.9	21.5	25.5
E_a^{HO}	32.9	33.3	37.0	37.6	35.3	26.9	30.9

[a] Units: kJ·mol^{-1}. Methyl acrylate propagation E_a obtained from PLP-SEC: 17.7 kJ·mol^{-1}. ZPVE values were calculated using UB3LYP/6-31G(d) with a scale factor of 0.9806. ZPVE(AD1) = 4.4 kJ·mol^{-1}; ZPVE(AD2) = 3.5 kJ·mol^{-1}; ZPVE(AD3) = 3.2 kJ·mol^{-1}.

calculated AD1 values at 298 K, which is consistent with the lower stability and the enhanced reactivity of a primary radical compared to a secondary (methyl acrylate) or tertiary (methyl methacrylate) radical.

Although calculations involving additional acrylate radicals are warranted before generalization is possible, we conclude that MPWB1K/6-31G(d,p) is an attractive method for obtaining results for acrylate polymerization with quantitative accuracy.

3.3. Low Frequency Treatment. In order to carry out the one-dimensional hindered rotation treatment, the sensitivity of the potential energy profiles to the step size and the level of theory was explored. Step sizes of 10° and 30° were both used for the methyl methacrylate AD1 reaction. Comparison of the data and their Fourier fits is provided in Figure 7. It is clear that the Fourier fits are nearly identical, and thus the properties calculated based on these scans would be the same. The agreement between the fits based on step sizes of 10° and 30° was similar for both the monomeric radical and the transition state. Therefore, the more coarse step size of 30° was used for all subsequent calculations.

Three ab initio methods (unrestricted B3LYP/6-31G(d), HF/6-31G(d), and HF/3-21G) and two semiempirical methods (AM1 and PM3) were used to carry out potential energy scans, and the results were compared. Potential energy scans of methyl methacrylate monomer based on these five methods are shown in Figure 8. For symmetric tops, these methods afford similar potential energy shapes, but the barrier heights are different by as much as 30 kJ·mol^{-1}. For asymmetric tops as shown in Figure 8c, B3LYP/6-31G(d) and HF/6-31G(d) have similar shapes and barrier heights, but the other three methods are different in both shape and barrier height. These results show that smaller basis sets and semiempirical methods are not a viable option for investigating methyl methacrylate polymerization. Therefore, all of the internal rotor partition functions in this research were calculated based on potential energy scans with unrestricted B3LYP/6-31G(d). It is also interesting to note that the barrier height is not only determined by the type of rotating group, but it also depends on the environment where the group is located. For example, the barrier height of the CH_3 group defined as D4 in Figure 4 is about 3 kJ·mol^{-1} lower than that defined as D1. It is attractive to have a "general" barrier height for a type of group because of the prevalence of repeating groups in polymerization chemistry, so that the treatment of internal rotations can be greatly simplified. However, analysis

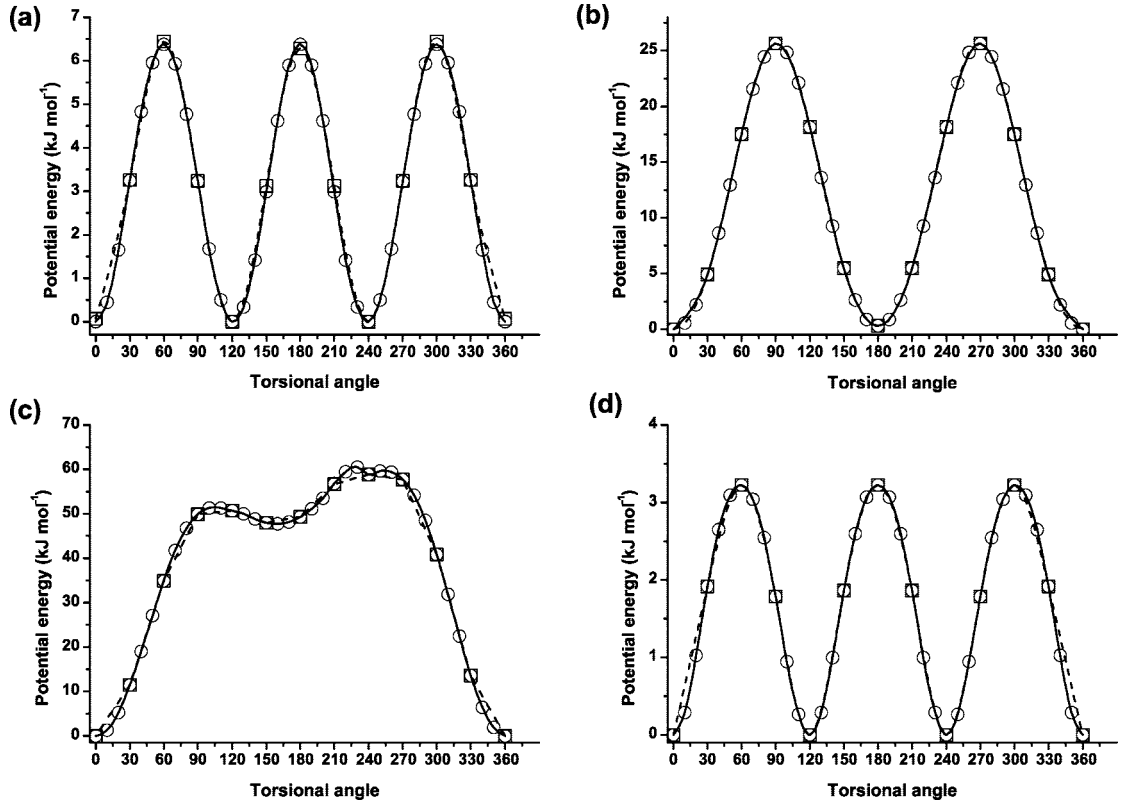

Figure 7. Potential energy scans for all the dihedrals defined for methyl methacrylate monomer in Figure 4: (a) D1, (b) D2, (c) D3, and (d) D4 at intervals of 10° (circles, solid line) and 30° (squares, dashed line) using unrestricted B3LYP/6-31G(d).

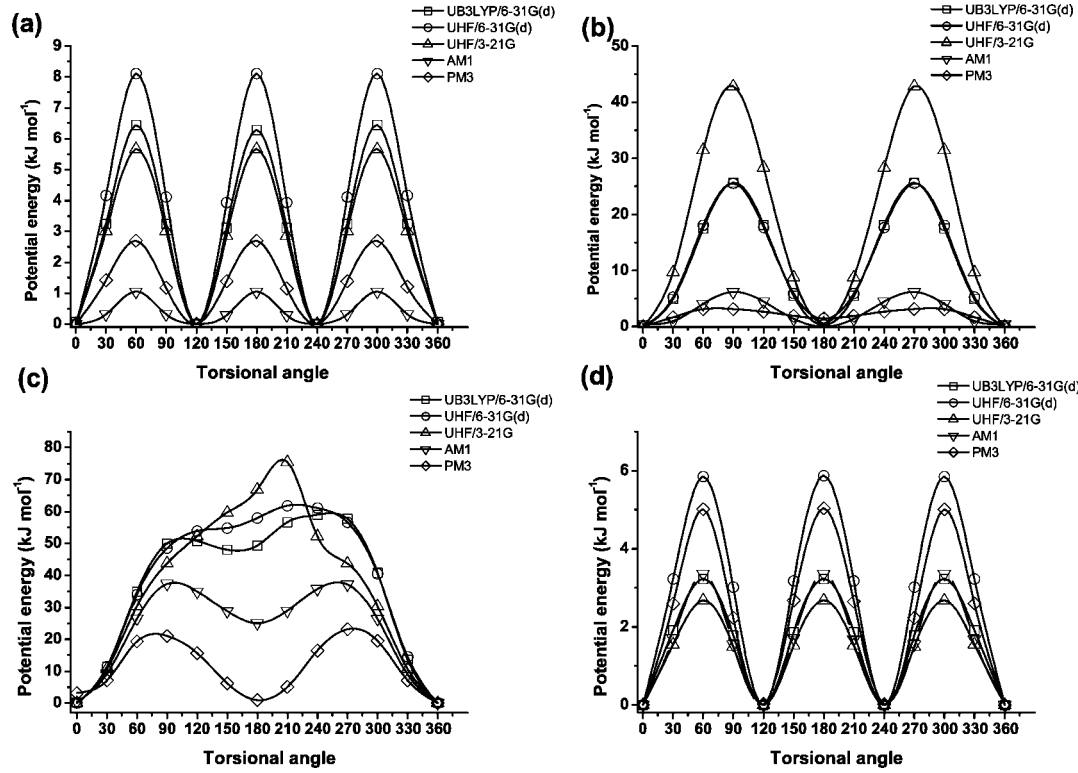

Figure 8. Comparison of potential energy scans for the dihedral angles of methyl methacrylate monomer using various methods. The dihedrals are defined as in Figure 4: (a) D1, (b) D2, (c) D3, and (d) D4.

of each of the rotating tops in the monomer, radicals, and transition states showed that it is not quantitatively accurate for methyl methacrylate and methyl acrylate polymerization to assign a single barrier height for a type of rotating top since the rotation is inevitably influenced by its surrounding groups.

3.4. Kinetics. On the basis of geometries optimized using unrestricted B3LYP/6-31G(d), frequencies calculated using B3LYP/6-31G(d) and electronic energies calculated using MPWB1K/6-31G(d,p), rate coefficients were calculated on the basis of eq 3 from 298.15 to 800 K for both methyl methacrylate

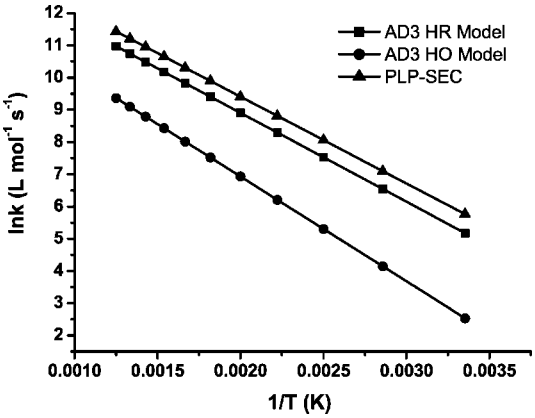

Figure 9. Plot of ln k versus $1/T$ for methyl methacrylate propagation over a temperature range of 298.15 to 800 K. The A and E_a values regressed from this plot are listed in Table 4.

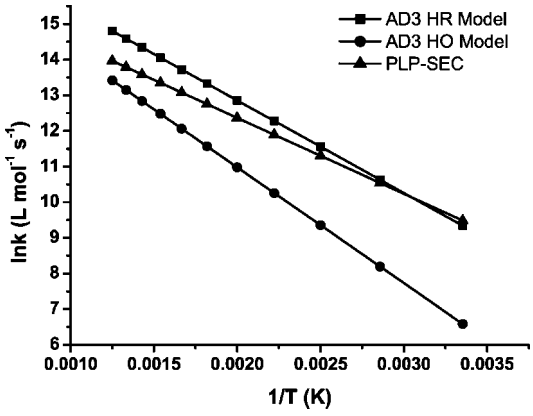

Figure 10. Plot of ln k versus $1/T$ for methyl acrylate propagation over a temperature range of 298.15 to 800 K. The A and E_a values regressed from this plot are listed in Table 5.

and methyl acrylate from AD1 to AD3. Kinetic parameters, A and E_a, were then regressed from a plot of ln k versus $1/T$ as shown in Figures 9 and 10 for methyl methacrylate and methyl acrylate, respectively. The impact of the one-dimensional HR treatment was explored by comparing the A and E_a values for both the HO and HR models. The rate coefficients were based on the lowest energy conformers for the reactants, although a range of rate coefficients would actually be expected based on conversion of reactants of many possible low energy conformations. The frequency factors and activation energies for methyl methacrylate propagation are summarized in Table 4, and those for methyl acrylate propagation are compiled in Table 5. It is clear from these results that treating low frequencies using the one-dimensional internal rotation model has an effect on both the activation energy and the frequency factor values. The calculated frequency factors are always higher than those calculated with the HO model, as shown in Tables 4 and 5, which is consistent with the data of Heuts and Gilbert[23] and Van Cauter et al.[24] Van Cauter and co-workers rationalized this in a straightforward manner by noting that, because the rotation about the transition state bond is taken into account, sampling more conformers, $Q^{\ddagger}$ increases and thus A increases. It is perhaps surprising then that calculated frequency factors based on the internal rotation model have also been reported to be lower than those based on the HO model.[25] For methyl methacrylate, the difference in E_a between the HO model and the internal rotation model for each reaction is about 4 kJ·mol^{-1}, which translates into a factor of 4 in k_p at 50 °C. The frequency factors based on the one-dimensional internal rotation model are higher than those based on the HO model for both methyl methacrylate and methyl acrylate: the ratio of A^{HR}/A^{HO} varies from 2.8 to 10.5 for methyl methacrylate, and for methyl acrylate, the ratio varies from 1.9 to 7.4. The activation energies calculated based on the one-dimensional internal rotation model are not uniformly higher or lower than those based on the HO model: for methyl methacrylate, the difference varies from −4.1 kJ·mol^{-1} to 4.1 kJ·mol^{-1}, while, for methyl acrylate, the difference varies from −5.4 kJ·mol^{-1} to 0.9 kJ·mol^{-1}. The best agreement between the calculated results and the experimental values for both monomers is for AD3 using the one-dimensional internal rotation model: for methyl methacrylate, E_a differs by only 0.3 kJ·mol^{-1}, and the frequency factor ratio ($A^{HR,\,AD3}/A^{PLP}$) is 0.6; for methyl acrylate, E_a differs by 3.8 kJ·mol^{-1} and the frequency factor ratio is 3.6. Overall, the k_p results from the HR model are in better agreement with the experimental data than the results from the HO model, as shown in Figures 9 and 10.

Increasing the radical chain length from one to three results in a moderate increase in the k_p values for both methyl methacrylate and methyl acrylate. The activation energies generally decrease as the chain length is increased for both monomers, with a more marked drop as the chain length increases from two to three. It is interesting to compare these trends with the experimental measurements of Heuts and Russell,[48] who drew on the results of Fischer and Radom for the first propagation step. They report that E_a is insensitive to chain length for methyl methacrylate. The trend reported for methyl acrylate is not relevant since the small molecule data of Fischer and Radom was not actually for a methyl acrylate radical. How reaction rate varies with increasing radical chain length is dependent on the properties of the radical and monomer.[48,49] For example, in research by Van Cauter and co-workers on ethylene propagation reaction, the addition rate constant decreases with increasing radical size,[24] while, in

TABLE 4: Frequency Factors (A: L·mol^{-1}·s^{-1}), Activation Energies (E_a: kJ·mol^{-1}) and Rate Constants (k_p: L·mol^{-1}·s^{-1}) at 50 °C for Methyl Methacrylate Propagation Calculated As a Function of Chain Length (AD1−AD3 in Figure 2) Using Geometries Optimized with Unrestricted B3LYP/6-31G(d) and Single-Point E_e Calculations Using MPWB1K/6-31G(d,p)[a]

	HR model			HO model				
	A	E_a	k_p	A	E_a	k_p	A^{HR}/A^{HO}	$E_a^{HR} - E_a^{HO}$
AD1	3.72×10^6	27.7	1.24×10^2	4.68×10^5	24.0	6.17×10^1	7.9	3.7
AD2	7.41×10^6	28.0	2.21×10^2	7.08×10^5	23.9	9.70×10^1	10.5	4.1
AD3	1.55×10^6	22.7	3.32×10^2	5.50×10^5	26.8	2.56×10^1	2.8	−4.1

	A	E_a	k_p	$A^{HR,AD3}/A^{PLP}$	$E_a^{HR,AD3} - E_a^{PLP}$
PLP-SEC	2.67×10^6	22.4	6.39×10^2	0.6	0.3

[a] A and E_a were regressed on the basis of k_p values from 298.15 to 800 K. Plots of ln k versus $1/T$ are shown in Figure 9.

TABLE 5: Frequency Factors (A: L·mol^{-1}·s^{-1}), Activation Energies (E_a: kJ·mol^{-1}) and Rate Constants (k_p: L·mol^{-1}·s^{-1}) at 50 °C for Methyl Acrylate Propagation Calculated As a Function of Chain Length (AD1−AD3 in Figure 2) Using Geometries Optimized with Unrestricted B3LYP/6-31G(d) and Single-Point E_e Calculations Using MPWB1K/6-31G(d,p)[a]

	HR model			HO model				
	A	E_a	k_p	A	E_a	k_p	A^{HR}/A^{HO}	$E_a^{HR} - E_a^{HO}$
AD1	7.24×10^7	26.4	3.91×10^3	9.77×10^6	25.5	7.38×10^2	7.4	0.9
AD2	6.31×10^7	22.8	1.30×10^4	1.70×10^7	22.4	4.07×10^3	3.7	0.4
AD3	6.03×10^7	21.5	2.02×10^4	3.16×10^7	26.9	1.42×10^3	1.9	−5.4

	A	E_a	k_p	$A^{HR,AD3}/A^{PLP}$	$E_a^{HR,AD3} - E_a^{PLP}$
PLP-SEC	1.66×10^7	17.7	2.29×10^4	3.6	3.8

[a] A and E_a were regressed on the basis of k_p values from 298.15 to 800 K. Plots of ln k versus $1/T$ are shown in Figure 10.

research by Izgorodina and Coote on methyl acrylonitrile and vinyl chloride, the rate constants increase with increasing radical size.[25]

Because computational time and resources prohibited going to chain lengths longer than four in the radical product, it is not possible to assess whether the predicted A, E_a, and k_p values have reached an asymptotic value. However, the excellent agreement with the experimental data and the diminishing impact of units far from the reactive center suggest that it is reasonable to use addition of a trimeric radical to monomer to predict rate coefficients for propagation of methyl methacrylate and methyl acrylate.

3.5. Solvation Model Results. The experimental data were determined from bulk polymerization, while the predicted results were based on calculations in a vacuum. It has been shown in previous research that kinetic parameters for free radical polymerization are not sensitive to the presence of solvent unless a high polarity solvent is used,[23,50] so it is reasonable that our calculated results were in excellent agreement with experiment. However, to probe this further, a PCM was used to study the influence of solvent on the conformation of the transition state and the kinetic parameters. "*SCRF(PCM,Read)*" with "*EPS* = 6.32" were used as keywords in Gaussian 03 to conduct this analysis for methyl methacrylate, and "*EPS* = 7.03" was used as a keyword for methyl acrylate. Comparison of the results with those from vacuum calculations reveals that the conformations of the reactants and the transition state are not affected strongly. For methyl methacrylate AD3 TS, the bond lengths (including the bond defining the transition state) differed by less than 0.001 Å, and the angles differed by less than 0.5°. The difference in the E_a value for methyl methacrylate AD3 was 1.9 kJ·mol^{-1}. For methyl acrylate AD3 TS, the bond lengths (including the bond defining the transition state) differed by less than 0.001 Å, and the angles differed by less than 0.3°. The difference in the AD3 E_a value was 1.0 kJ·mol^{-1}.

4. Conclusion

A computational methodology based on quantum chemistry and transition state theory has been used to calculate kinetic parameters for methyl methacrylate and methyl acrylate propagation reactions. A combination of conventional geometry optimization and relaxed potential energy scans for each single bond and the bond defining the transition state was used in order to locate "global" minimum conformations. Three DFT methods with different basis sets were evaluated for calculating activation energies of methyl methacrylate addition reactions, and the results showed that MPWB1K/6-31G(d,p) provided values that were the closest to and in very good agreement with experimental data. This choice of method and basis set was also verified for methyl acrylate. The addition reactions of monomeric, dimeric, and trimeric radicals to monomer were analyzed for both methyl methacrylate and methyl acrylate, and the results showed that the addition of a trimeric radical to monomer offered results that were the most consistent with experimental data. Calculations employing a solvation model revealed that the solvent effect was not marked for either methyl methacrylate or methyl acrylate propagation reactions. Two different treatments were used in the calculation of the contribution of low frequencies to the kinetic parameters. The results based on the one-dimensional internal rotation model are closer to experimental data than those based on the HO model.

Acknowledgment. We acknowledge the Inter-American Materials Collaboration Program of the National Science Foundation (DMR-0303435) for financial support. Supercomputer resources from NCSA (TG-CTS050021) are also gratefully acknowledged. We would also like to thank Dr. Karen Van Cauter and Dr. Veronique Van Speybroeck for very helpful discussions regarding the treatment of internal rotations.

References and Notes

(1) Grady, M. C.; Simonsick, W. J.; Hutchinson, R. A. *Macromol. Symp.* **2002**, *182*, 149.
(2) Reisch, R. *Chem. Eng. News* **1993**, *71*, 34.
(3) Adamsons, K.; Blackman, G.; Gregorovich, B.; Lin, L.; Matheson, R. *Prog. Org. Coat.* **1998**, *34*, 64.
(4) Hakim, M.; Verhoeven, V.; McManus, N. T.; Debe, M. A.; Penlidis, A. *J. Appl. Polym. Sci.* **2000**, *77*, 1156.
(5) Plessis, C.; Arzamendi, G.; Leiza, J. R.; Schoonbrood, H. A.; Charmot, D.; Asua, J. M. *Macromolecules* **2000**, *33*, 4.
(6) McCord, E. F.; Shaw, W. H.; Hutchinson, R. A. *Macromolecules* **1997**, *30*, 246.
(7) Ahmad, N. M.; Heatley, F.; Lovell, P. A. *Macromolecules* **1998**, *31*, 2822.
(8) Beuermann, S.; Buback, M.; Davis, T. *Macromol. Chem. Phys.* **1997**, *198*, 1545.
(9) Buback, M.; Kurz, C.; Schmaltz, C. *Macromol. Chem. Phys.* **1998**, *199*, 1721.
(10) Beuermann, S.; Paquet, J.; McMinn, J. *Macromolecules* **1996**, *29*, 4206.
(11) Beuermann, S.; Buback, M.; Gilbert, R. G. *Macromol. Chem. Phys.* **2000**, *201*, 1355.
(12) Beuermann, S.; Buback, M.; Schmaltz, C. *Ind. Eng. Chem. Res.* **1999**, *38*, 3338.
(13) Buback, M.; Kowollik, C. *Macromolecules* **1998**, *31*, 3211.
(14) Beuermann, S.; Buback, M. *Ind. Eng. Chem. Res.* **1999**, *200*, 1764.
(15) Buback, M.; Feldermann, A.; Barner-Kowollik, C. *Macromolecules* **2001**, *34*, 5439.
(16) Hutchinson, R. A.; Paquet, D. A.; Beuermann, S.; McMinn, J. H. *Ind. Eng. Chem. Res.* **1998**, *37*, 3567.
(17) Yamada, B.; Azukzawa, M.; Yamazoe, H.; Hill, D.; Pomery, P. J. *Polymer* **2000**, *41*, 5611.
(18) Peck, A. N.; Hutchinson, R. A. *Macromolecules* **2004**, *37*, 5944.
(19) Fischer, H.; Radom, L. *Angew. Chem., Int. Ed.* **2001**, *40*, 1340.
(20) Irikura, K. K. *Computational Thermochemistry: Prediction and Estimation of Molecular Thermodynamics*, 1st ed.; American Chemical Society: Washington, DC, 1998.

(21) Hehre, W. J.; Radom, L.; Schleyer, P. V. R. *Ab Initio Molecular Orbital Theory*, 1st ed.; Wiley: New York, 1986.
(22) Pilar, F. L. *Elementary Quantum Chemistry*, 2nd ed.; McGraw-Hill: Singapore, 1990.
(23) Heuts, J. P.; Gilbert, R. G. *Macromolecules* **1995**, *28*, 8771.
(24) Cauter, K. V.; Speybroeck, V. V.; Vansteenkiste, P.; Reyniers, M. F.; Waroquier, M. *ChemPhysChem* **2006**, *7*, 131.
(25) Izgorodina, E. I.; Coote, M. L. *Chem. Phys.* **2006**, *324*, 96.
(26) Huang, D. M.; Monteiro, M. J.; Gilbert, R. G. *Macromolecules* **1998**, *31*, 5175.
(27) Wong, M. W.; Radom, L. *J. Phys. Chem. A* **1998**, *102*, 2237.
(28) Coote, M. L. *J. Phys. Chem. A* **2005**, *109*, 1230.
(29) Frisch, M. J.; Trucks, G. W.; Schlegel, H. B.; Scuseria, G. E.; Robb, M. A.; Cheeseman, J. R.; Montgomery, J. A.; Vreven, J. T.; Kudin, K. N.; Burant, J. C.; Millam, J. M.; Iyengar, S. S.; Tomasi, J.; Barone, V.; Mennucci, B.; Cossi, M.; Scalmani, G.; Rega, N.; Petersson, G. A.; Nakatsuji, H.; Hada, M.; Ehara, M.; Toyota, K.; Fukuda, R.; Hasegawa, J.; Ishida, M.; Nakajima, T.; Honda, Y.; Kitao, O.; Nakai, H.; Klene, M.; Li, X.; Knox, J. E.; Hratchian, H. P.; Cross, J. B.; Adamo, C.; Jaramillo, J.; Gomperts, R.; Stratmann, R. E.; Yazyev, O.; Austin, A. J.; Cammi, R.; Pomelli, C.; Ochterski, J. W.; Ayala, P. Y.; Morokuma, K.; Voth, G. A.; Salvador, P.; Dannenberg, J. J.; Zakrzewski, V. G.; Dapprich, S.; Daniels, A. D.; Strain, M. C.; Farkas, O.; Malick, D. K.; Rabuck, A. D.; Raghavachari, K.; Foresman, J. B.; Ortiz, J. V.; Cui, Q.; Baboul, A. G.; Clifford, S.; Cioslowski, J.; Stefanov, B. B.; Liu, G.; Liashenko, A.; Piskorz, P.; Komaromi, I.; Martin, R. L.; Fox, D. J.; Keith, T.; Al-Laham, M. A.; Peng, C. Y.; Nanayakkara, A.; Challacombe, M.; Gill, P. M. W.; Johnson, B.; Chen, W.; Wong, M. W.; Gonzalez, C.; Pople, J. A. *Gaussian 03*, revision c.02; Gaussian, Inc.: Wallingford CT, 2004.
(30) Schlegel, H. B. *J. Comput. Chem.* **1982**, *3*, 214.
(31) Foresman, J. B. *Exploring Chemistry with Electronic Structure Methods*, 1st ed.; Gaussian Inc.: Pittsburgh, PA, 2002.
(32) Peng, C.; Avala, P. Y.; Schelegel, H. B. *J. Comput. Chem.* **1996**, *317*, 49.
(33) Scott, A. P.; Radom, L. *J. Phys. Chem.* **1996**, *100*, 16502.
(34) Zhao, Y.; Truhlar, D. G. *J. Phys. Chem. A* **2004**, *108*, 6908.
(35) Becke, A. D. *J. Chem. Phys.* **1996**, *104*, 1040.
(36) Cances, E.; Mennucci, B.; Tomasi, J. *J. Chem. Phys.* **1997**, *107*, 3032.
(37) Speight, J. G. *Lange's Handbook of Chemistry*, 16th ed.; McGraw-Hill: NewYork, 2004.
(38) Pfaendtner, J.; Broadbelt, L. J. *Chem. Eng. Sci.* **2007**, *62*, 5232.
(39) McQuarrie, D. A.; Simon, J. D. *Molecular Thermodynamics*, 1st ed.; University Science Books: Sausalito, CA, 1999.
(40) Pfaendtner, J.; Yu, X.; Broadbelt, L. J. *J. Phys. Chem. A* **2006**, *110*, 10863.
(41) Pfaendtner, J.; Broadbelt, L. J. *ChemPhysChem* **2007**, *8*, 1969.
(42) McClurg, R. B.; Flagan, R. C.; Goddard, W. A. *J. Comput. Chem.* **1997**, *106* (16), 6675.
(43) Truhlar, D. G. *J. Comput. Chem.* **1991**, *12* (2), 266.
(44) East, A. L. L.; Radom, L. *J. Chem. Phys.* **1997**, *106* (16), 6655.
(45) Balint-Kurti, G. G.; Dixon, R. N.; Marston, C. C. *Int. Rev. Phys. Chem.* **1992**, *11* (2), 317.
(46) Pfaendtner, J.; Yu, X.; Broadbelt, L. J. *calck*, version 1.0, available for use free of charge by contacting Linda J. Broadbelt.
(47) Pfaendtner, J.; Yu, X.; Broadbelt, L. J. *Theor. Chem. Acc.* **2007**, *118*, 881.
(48) Heuts, J. P.; Russell, G. T. *Eur. Polym. J.* **2006**, *42*, 3.
(49) Gridnev, A. A.; Ittel, S. D. *Macromolecules* **1996**, *29*, 5864.
(50) Thickett, S. C.; Gilbert, R. G. *Polymer* **2004**, *45*, 6993.

JP800643A